

RESEARCH

Open Access



# Dysregulated expression levels of *APH1B* in peripheral blood are associated with brain atrophy and amyloid- $\beta$ deposition in Alzheimer's disease

Young Ho Park<sup>1</sup> , Jung-Min Pyun<sup>2</sup>, Angela Hodges<sup>3</sup>, Jae-Won Jang<sup>4</sup>, Paula J. Bice<sup>5</sup>, SangYun Kim<sup>1</sup>, Andrew J. Saykin<sup>5,6</sup> and Kwangsik Nho<sup>5,7\*</sup> for the AddNeuroMed consortium and the Alzheimer's Disease Neuroimaging Initiative

## Abstract

**Background:** The interaction between the brain and periphery might play a crucial role in the development of Alzheimer's disease (AD).

**Methods:** Using blood transcriptomic profile data from two independent AD cohorts, we performed expression quantitative trait locus (*cis*-eQTL) analysis of 29 significant genetic loci from a recent large-scale genome-wide association study to investigate the effects of the AD genetic variants on gene expression levels and identify their potential target genes. We then performed differential gene expression analysis of identified AD target genes and linear regression analysis to evaluate the association of differentially expressed genes with neuroimaging biomarkers.

**Results:** A *cis*-eQTL analysis identified and replicated significant associations in seven genes (*APH1B*, *BIN1*, *FCER1G*, *GATS*, *MS4A6A*, *RABEP1*, *TRIM4*). *APH1B* expression levels in the blood increased in AD and were associated with entorhinal cortical thickness and global cortical amyloid- $\beta$  deposition.

**Conclusion:** An integrative analysis of genetics, blood-based transcriptomic profiles, and imaging biomarkers suggests that *APH1B* expression levels in the blood might play a role in the pathogenesis of AD.

**Keywords:** Alzheimer's disease, Transcriptome, Blood, Expression quantitative trait locus, Genome-wide association study, Expression, Imaging

## Introduction

Alzheimer's disease (AD) has a strong genetic component with high heritability (~70%) [1]. Over the last 10 years, more than 30 genes/loci have been identified as associated with AD by large-scale genome-wide association

studies (GWASs) and sequencing data analysis [2]. However, most of the GWAS signals are located in noncoding regions of the genome, and their functional impact on AD is as yet poorly understood [3].

The interaction between the brain and periphery might play a crucial role in the development and pathogenesis of AD [4]. AD is classically regarded as a brain disorder. Despite the debate, an imbalance between production and clearance of amyloid- $\beta$  (A $\beta$ ) in the brain is a very early, often initiating, factor in AD [5]. However, increasing experimental and epidemiological evidence has

\*Correspondence: knho@iu.edu

<sup>5</sup> Department of Radiology and Imaging Sciences, and the Indiana Alzheimer Disease Center, Center for Neuroimaging, Indiana University School of Medicine, Indianapolis, IN, USA  
Full list of author information is available at the end of the article



© The Author(s) 2021. **Open Access** This article is licensed under a Creative Commons Attribution 4.0 International License, which permits use, sharing, adaptation, distribution and reproduction in any medium or format, as long as you give appropriate credit to the original author(s) and the source, provide a link to the Creative Commons licence, and indicate if changes were made. The images or other third party material in this article are included in the article's Creative Commons licence, unless indicated otherwise in a credit line to the material. If material is not included in the article's Creative Commons licence and your intended use is not permitted by statutory regulation or exceeds the permitted use, you will need to obtain permission directly from the copyright holder. To view a copy of this licence, visit <http://creativecommons.org/licenses/by/4.0/>. The Creative Commons Public Domain Dedication waiver (<http://creativecommons.org/publicdomain/zero/1.0/>) applies to the data made available in this article, unless otherwise stated in a credit line to the data.

suggested that manifestations of AD extend beyond the brain [4]. For example, A $\beta$  is produced not only in brain cells but also in peripheral organs and tissues including the liver, muscles, and various blood and endothelial cells [6]. Furthermore, the CNS and peripheral pools of A $\beta$  can interact; some A $\beta$  peptides in the CNS are cleared by phagocytosis or proteolytic degradation, whereas others are released into the blood [4]. Some A $\beta$  peptides in the blood are phagocytosed by peripheral immune cells; some are degraded by A $\beta$ -degrading enzymes, and some are transported by carriers to peripheral organs or tissues where they are degraded or excreted [4]. Considering there is a close interaction of A $\beta$  metabolism between the brain and the periphery and trait-associated single nucleotide polymorphisms (SNPs) are likely to be expression quantitative trait loci (*cis*-eQTL) [7], the integrative analysis of genetics, blood-based transcriptomic profiles, and neuroimaging AD biomarkers could provide an opportunity for assessing the complex interplay between the brain and the periphery in the pathogenesis of AD [8].

In this study, we performed a *cis*-eQTL analysis of significant AD-associated SNPs from a recent AD GWAS meta-analysis [3] to investigate the effects of the AD SNPs on blood gene expression levels and identify their potential target genes using blood transcriptomic profile data from two independent AD cohorts. We then performed gene-set enrichment and differential gene expression analyses of identified target genes and evaluated associations of differentially expressed genes with neuroimaging biomarkers for AD and plasma protein levels.

## Methods

### Participants

Individuals used in the study were non-Hispanic Caucasian participants (AD, mild cognitive impairment (MCI), and cognitively normal older adults (CN)) from the Alzheimer's Disease Neuroimaging Initiative (ADNI) and AddNeuroMed cohorts as discovery and replication samples, respectively. The ADNI was launched in 2003 as a public-private partnership, led by Principal Investigator Dr. Michael W. Weiner [9]. The primary goal of ADNI has been to test whether serial MRI, PET, other biological markers, and clinical and neuropsychological assessment can be combined to accurately capture the progression of MCI and early AD. The AddNeuroMed is a cross-European, public/private consortium developed for AD biomarker discovery [10]. The ADNI participants were recruited in North America, whereas the AddNeuroMed participants were recruited in Europe. In both cohorts, participants were categorized into three diagnostic groups (CN, MCI, AD). AD was diagnosed clinically according to the NINCDS/ADRDA criteria for probable AD in ADNI and AddNeuroMed [11]. MCI was

diagnosed when there was objective memory impairment but without meeting the criteria for dementia [9, 10]. Written informed consent was obtained at the time of enrollment and included permission for analysis and data sharing. The protocol and informed consent forms were approved by the Institutional Review Board at each participating site.

### Genotyping and imputation

Genome-wide genotyping was performed using Illumina GWAS array platforms (Illumina Human610-Quad BeadChip, Illumina HumanOmni Express BeadChip, and Illumina HumanOmni 2.5 M BeadChip) [12, 13]. *APOE* genotyping was separately conducted [12]. Using PLINK 1.9 ([www.cog-genomics.org/plink2/](http://www.cog-genomics.org/plink2/)) [14], we then performed standard quality control (QC) procedures for samples and SNPs as described previously [15]: (1) for SNP, SNP call rate < 95%, Hardy-Weinberg *P*-value <  $1 \times 10^{-6}$ , and minor allele frequency (MAF) < 1%; (2) for sample, sex inconsistencies, and sample call rate < 95%. In order to prevent spurious associations due to population stratification, we used multidimensional scaling analysis to select only non-Hispanic participants of European ancestry that clustered with HapMap CEU (Utah residents with Northern and Western European ancestry from the CEPH collection) or TSI (Toscani in Italia) populations [16, 17]. After QC procedures (Supplementary Fig. 1), because these cohorts used different genotyping platforms, we imputed un-genotyped SNPs separately in each platform using MaCH with the Haplotype Reference Consortium data as a reference panel [18, 19].

### Blood-based RNA expression microarray profiling

The PAXgene Blood RNA Kit (Qiagen Inc., Valencia, CA, USA) was used to purify total RNA from the whole blood [12, 20]. The Affymetrix Human Genome U219 Array (Affymetrix, Santa Clara, CA, USA) and the Illumina Human HT-12 v3 Expression BeadChips (Illumina Inc., San Diego, CA, USA) were used in ADNI and AddNeuroMed, respectively, for expression profiling. All probe sets were mapped to the human genome reference sequence (hg19). Raw expression values were preprocessed with the robust multi-chip average normalization method in ADNI [21] and the robust spline normalization method in AddNeuroMed [22]. We investigated discrepancies between the reported sex and sex determined from sex-specific gene expression data, including *XIST* and *USP9Y*. We also checked whether SNP genotypes were matched with genotypes predicted from gene expression data [23]. After QC (Supplementary Fig. 2), the RNA expression profiles, which contained 21,150 probes in ADNI and 5141 probes in AddNeuroMed, were

pre-adjusted with batch effects and RNA integrity number values using linear regression analysis.

#### Identification of target genes of GWAS SNPs from eQTL analysis

As AD-associated SNPs, we used 29 independent SNPs from 29 distinct loci that showed genome-wide significant associations ( $P < 5 \times 10^{-8}$ ) in a recent AD GWAS meta-analysis [3]. Then, we selected genes that were located within  $\pm 1$  Mbp of 29 genome-wide significant SNPs and performed a *cis*-eQTL analysis using imputed GWAS and blood gene expression data to identify target genes as significantly associated with 29 genome-wide significant SNPs (false discovery rate (FDR)-corrected  $P < 0.05$ ) [24] in ADNI and AddNeuroMed as discovery and replication samples, respectively.

#### Pathway-based enrichment and differential gene expression analyses

We performed gene-set enrichment analysis to identify the biological pathways of AD-relevant target genes that were identified in ADNI and replicated in AddNeuroMed using three categories (biological process, molecular function, and cellular component) of the Gene Ontology (GO) resource [25, 26] and Enrichr (<https://maayanlab.cloud/Enrichr/>) [27]. We selected significantly enriched terms (FDR-corrected  $P < 0.05$ ) that have at least 2 genes. We then performed an analysis of covariance (ANCOVA) and made violin plots to investigate which genes were differentially expressed between AD, MCI, and CN (FDR-corrected  $P < 0.05$ ) and examined whether the ADNI findings were replicated in AddNeuroMed. We used age and sex as covariates.

#### Assessment of the causal effect of differentially expressed genes on AD

We performed GWAS summary data-based Mendelian randomization (SMR) analysis [28] to assess the causal effect of differentially expressed genes on AD using eQTLGen data for peripheral blood [29] and a recent large-scale GWAS summary data for AD [3]. We also performed a HEIDI (heterogeneity in dependent instruments) test to distinguish pleiotropy from linkage [28].

#### Association of differentially expressed genes with neuroimaging AD biomarkers and plasma-based protein levels

Hippocampal volume and entorhinal cortical thickness were measured as MRI biomarkers from T1-weighted brain MRI scans using FreeSurfer version 5.1 ([surfer.nmr.mgh.harvard.edu](http://surfer.nmr.mgh.harvard.edu)) in both cohorts [30]. We performed a linear regression analysis to evaluate whether expression levels of differentially expressed genes were associated

with hippocampal volume and entorhinal cortical thickness in ADNI (FDR-corrected  $P < 0.05$ ) and to examine whether the ADNI findings were replicated in AddNeuroMed. We used age, sex, intracranial volumes, and MRI field strength as covariates. We also used a linear mixed model to jointly analyze the pooled individual imaging data from the ADNI and AddNeuroMed cohorts. Furthermore, global cortical amyloid deposition, as mean standardized uptake values, was measured as an amyloid PET biomarker using preprocessed (coregistered, averaged, standardized image and voxel size, uniform resolution) [ $^{18}$ F] florbetapir PET scans with a whole cerebellum reference region in ADNI [31]. We performed linear regression analysis to evaluate whether expression levels of the differentially expressed genes were associated with brain amyloid deposition (FDR-corrected  $P < 0.05$ ). We used age and sex as covariates. Amyloid biomarkers were not available in AddNeuroMed.

As plasma-based protein levels, 1001 proteins were measured using SOMAscan (SomaLogic, Inc., Boulder, CO, USA) Multiplexed Proteomic technology in the AddNeuroMed cohort [32]. We performed linear regression analysis to evaluate whether expression levels of differentially expressed genes were associated with plasma protein levels. We then performed ANCOVA to investigate which plasma proteins were differentially expressed between AD, MCI, and CN with age and sex as covariates.

#### Association of differentially expressed genes with progression of MCI to AD dementia

We assessed the hazard ratio of expression levels of differentially expressed genes using Cox regression analysis with the follow-up time as a time variable and progression of MCI to AD dementia during follow-up period up to 5 years as a status variable. Covariates included age and sex.

In this study, we used R version 3.6.3 ([R-project.org](http://R-project.org)) for analysis unless otherwise specified. All statistical tests are two-sided unless otherwise specified.

#### Results

A total of 1335 participants were included from two independent cohorts (661 from the ADNI and 674 from AddNeuroMed) in this study (Table 1). Using imputed GWAS and blood-based RNA gene expression data, we discovered that 29 genome-wide significant SNPs were eQTLs of 30 genes (*ADAMTS4*, *AIF1*, *APH1B*, *ARF4*, *AURKA*, *BIN1*, *CDS5*, *CHRNE*, *CNN2*, *CSTF1*, *EPHA1*, *FAM63B*, *FCER1G*, *GATS*, *HLA-DRB1*, *MS4A4A*, *MS4A6A*, *MYBBP1A*, *NDUFS2*, *NUP88*, *PVRIG*, *RABEP1*, *SCIMP*, *SLC24A4*, *TAF6*, *TAP2*, *TRIM4*, *ZCWPW1*, *ZKSCAN1*, *ZNF668*;

**Table 1** Demographics of study samples

Cohort	Diagnosis	N	Female (%)	Age at blood sample collection, mean (SD)	RIN, mean (SD)
ADNI (N=661)	CN	213	107 (50%)	76.4 (6.4)	6.91 (0.51)
	MCI	345	144 (42%)	73.2 (7.9)	6.98 (0.55)
	AD	103	38 (37%)	77.6 (7.8)	6.98 (0.64)
AddNeuroMed (N=674)	CN	243	147 (60%)	74.2 (6.6)	8.96 (0.73)
	MCI	208	120 (58%)	75.5 (6.5)	8.50 (0.59)
	AD	223	146 (65%)	76.8 (6.8)	8.43 (0.64)

The table was modified from a previous study [51]

Abbreviations: AD Alzheimer's disease; CN cognitively normal older adults; MCI mild cognitive impairment; RIN RNA integrity number; SD standard deviation

Supplementary Table 1) in ADNI and 15 genes (*APH1B*, *BIN1*, *CLPTM1*, *FCER1G*, *GATS*, *HLA-DQA1*, *HLA-DRA*, *HSPA6*, *ITGAX*, *MS4A6A*, *PILRB*, *RABEP1*, *RXRBB*, *SNRPD2*, *TRIM4*; Supplementary Table 2) in AddNeuroMed. Seven genes (*APH1B*, *BIN1*, *FCER1G*, *GATS*, *MS4A6A*, *RABEP1*, *TRIM4*) were identified in ADNI and replicated in AddNeuroMed after adjusting for multiple testing.

Gene-set enrichment analysis of these seven genes revealed five significant pathways (protein oligomerization, positive regulation of programmed cell death, positive regulation of apoptotic process, vesicle-mediated transport, and regulation of apoptotic process) in the category of GO biological process and one significant pathway (protein homodimerization activity) in the category of GO molecular function (Table 2). No significant pathways were identified in the category of GO cellular component.

In ADNI, differential gene expression analysis showed that expression levels of *APH1B* significantly increased in AD compared to CN (Supplementary Table 3) after adjusting for multiple testing, and this finding was replicated in AddNeuroMed (Fig. 1). In SMR analysis, we found that  $P_{SMR}$  of *APH1B* was  $1.21 \times 10^{-7}$ , which passed the experiment-wise significance threshold ( $P_{SMR} < 3.18 \times 10^{-6}$ ) and suggested the causal effect of

*APH1B* expression on AD.  $P_{HEIDI}$  of *APH1B* was 0.053, which also passed the HEIDI test ( $P_{HEIDI} \geq 0.05$ ).

In addition, expression levels of *APH1B* were significantly associated with hippocampal volume and entorhinal cortical thickness in ADNI but not in AddNeuroMed (Table 3 and Fig. 2). However, when the pooled individuals from the ADNI and AddNeuroMed cohorts were jointly analyzed using a linear mixed model, expression levels of *APH1B* were associated with entorhinal cortical thickness but not with hippocampal volume. Furthermore, expression levels of *APH1B* were significantly associated with global cortical amyloid deposition in ADNI (Table 3 and Fig. 2).

With regard to plasma-based protein levels, 331 participants were available in AddNeuroMed. Expression levels of *APH1B* were associated with plasma levels of neuropilin-1, tropomyosin receptor kinase A, growth hormone receptor, and apolipoprotein A1 (Table 4). Particularly, levels of growth hormone receptor were significantly decreased in AD and MCI compared to CN (Table 4).

In Cox regression analysis, we used 320 and 186 patients with MCI in ADNI and AddNeuroMed, respectively, after excluding MCI without follow-up data. Among them, 61 and 47 MCI patients converted to AD in ADNI and AddNeuroMed, respectively, within a 5-year period after baseline. The hazard ratio (95% confidence

**Table 2** Biological pathways identified in the enrichment analysis

Category	Pathway	Overlap	P-value	FDR-corrected P-value	Odds ratio	Gene
Biological process	Protein oligomerization	2/217	$2.37 \times 10^{-3}$	$7.81 \times 10^{-3}$	26.33	<i>FCER1G</i> , <i>TRIM4</i>
	Positive regulation of programmed cell death	2/257	$3.31 \times 10^{-3}$	$7.81 \times 10^{-3}$	22.23	<i>APH1B</i> , <i>BIN1</i>
	Positive regulation of the apoptotic process	2/307	$4.69 \times 10^{-3}$	$7.81 \times 10^{-3}$	18.61	<i>APH1B</i> , <i>BIN1</i>
	Vesicle-mediated transport	2/410	$8.22 \times 10^{-3}$	$1.03 \times 10^{-2}$	13.94	<i>BIN1</i> , <i>RABEP</i>
	Regulation of the apoptotic process	2/815	$3.04 \times 10^{-2}$	$3.04 \times 10^{-2}$	7.01	<i>APH1B</i> , <i>BIN1</i>
Molecular function	Protein homodimerization activity	2/664	$2.07 \times 10^{-2}$	$2.07 \times 10^{-2}$	8.61	<i>FCER1G</i> , <i>RABEP1</i>

Overlap means a ratio of the number of input genes to the number of genes associated with each biological pathway. P-values and odds ratios were obtained from Fisher's exact test

Abbreviation: FDR false discovery rate

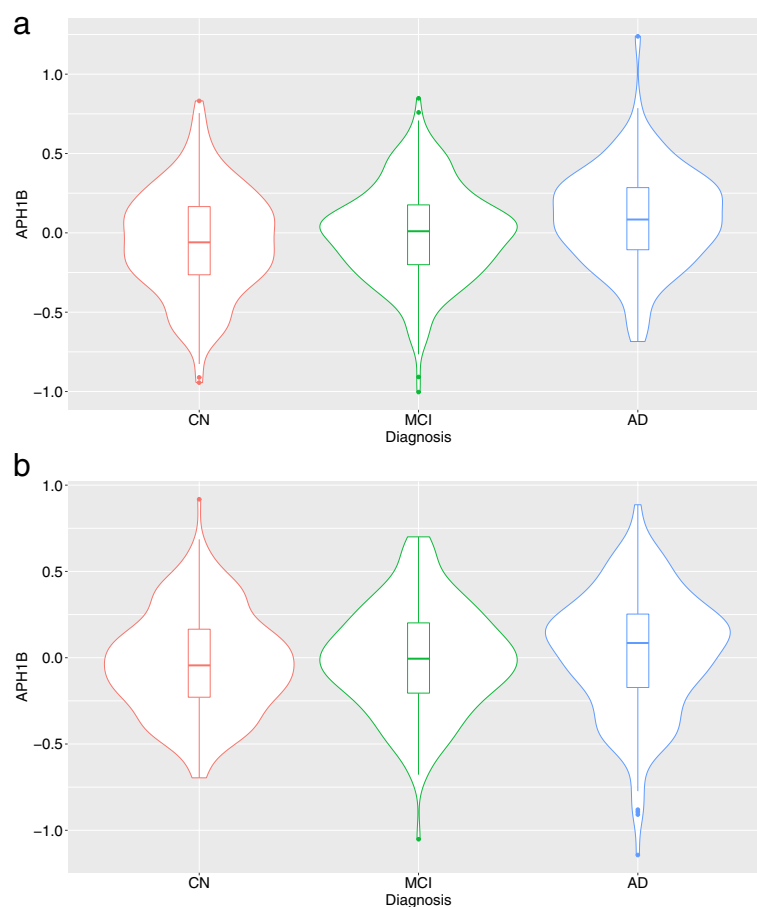


**Fig. 1** Violin plots for the blood expression levels of *APH1B* between CN, MCI, and AD. The violin plots show the probability density of the blood expression levels of *APH1B* as well as median and interquartile ranges in ADNI (a) and AddNeuroMed (b). The transcript identifier for *APH1B* was 11720068\_a\_at in ADNI and ILMN\_1767816 in AddNeuroMed, respectively. Abbreviation: AD, Alzheimer disease; ADNI, Alzheimer's Disease Neuroimaging Initiative; CN, cognitively normal older adults; MCI, mild cognitive impairment

interval) of expression levels of *APH1B* was 2.52 (1.02–6.25) in ADNI, whereas expression levels of *APH1B* were not significant in AddNeuroMed ( $HR=0.765$ ).

## Discussion

In this study, we identified and replicated seven target genes of 29 AD susceptibility SNPs of a recent large-scale GWAS by performing an eQTL analysis of blood transcriptomic profiles from two independent cohorts including AD, MCI, and CN. The biological pathways enriched in the seven genes included programmed cell death, protein oligomerization, and vesicle-mediated transport. Among the seven genes, expression levels of *APH1B* increased in the blood of AD patients and were associated with entorhinal cortical thickness; global cortical amyloid deposition; several plasma-based protein levels, including growth hormone receptors; and progression from MCI to AD dementia.

Programmed cell death or apoptosis, one of the biological pathways altered in peripheral blood from our study, has been commonly found in neurons and glial cells in AD [33]. Amyloid precursor protein intracellular domain (AICD), which is an amyloid precursor protein (APP)-derived cleavage product, was known to induce apoptosis in the pathogenesis of AD [34]. With respect to blood cells, the lymphocyte content of APP and apoptosis of lymphocytes are increased in patients with AD [35, 36]. The peripheral adaptive immune system including lymphocytes was reported to restrain AD pathology by clearance of A $\beta$  [37]. Protein oligomerization plays a crucial role in the pathogenesis of AD [38]. In blood, the oligomerization tendency of A $\beta$  is a diagnostic biomarker of AD [39] and is associated with neurodegenerative structural changes on MRI [40]. Vesicle-mediated transport includes various cellular transport processes using membrane-bounded vesicles. Previously, peripheral blood gene expression analysis showed that Fc-gamma

**Table 3** Association of the expression levels of *APH1B* with neuroimaging biomarkers in ADNI and AddNeuroMed

Cohort	Neuroimaging biomarker	Transcript ID	T-value	P-value	FDR-corrected P-value
ADNI	Entorhinal cortical thickness <sup>a</sup>	11720068_a_at	-2.85	$4.50 \times 10^{-3}$	$2.25 \times 10^{-2}$
		11740603_a_at	-2.36	$1.87 \times 10^{-2}$	$4.67 \times 10^{-2}$
		11740602_s_at	-0.482	$6.30 \times 10^{-1}$	$7.74 \times 10^{-1}$
		11720067_a_at	0.389	$6.98 \times 10^{-1}$	$7.74 \times 10^{-1}$
		11740601_a_at	0.287	$7.74 \times 10^{-1}$	$7.74 \times 10^{-1}$
	Hippocampal volume <sup>a</sup>	11720068_a_at	-2.69	$7.40 \times 10^{-3}$	$3.70 \times 10^{-2}$
		11740603_a_at	-1.96	$5.06 \times 10^{-2}$	$1.27 \times 10^{-1}$
		11740602_s_at	-0.104	$9.17 \times 10^{-1}$	$9.69 \times 10^{-1}$
		11720067_a_at	-0.0969	$9.23 \times 10^{-1}$	$9.69 \times 10^{-1}$
		11740601_a_at	0.0384	$9.69 \times 10^{-1}$	$9.69 \times 10^{-1}$
	Averaged cortical uptake of [ <sup>18</sup> F] florbetapir PET <sup>b</sup>	11720068_a_at	3.15	$1.71 \times 10^{-3}$	$8.54 \times 10^{-3}$
		11740603_a_at	2.64	$8.51 \times 10^{-3}$	$2.13 \times 10^{-2}$
		11740602_s_at	1.01	$3.14 \times 10^{-1}$	$5.23 \times 10^{-1}$
AddNeuroMed	Entorhinal cortical thickness <sup>c</sup>	ILMN_1767816	-0.761	$4.47 \times 10^{-1}$	N/A
		ILMN_1767816	0.454	$6.50 \times 10^{-1}$	N/A
	Hippocampal volume <sup>c</sup>	ILMN_1767816	0.454	$6.50 \times 10^{-1}$	N/A
		ILMN_1767816	0.454	$6.50 \times 10^{-1}$	N/A
ADNI and AddNeuroMed	Entorhinal cortical thickness <sup>d</sup>	11720068_a_at	-2.96	$3.18 \times 10^{-3}$	N/A
	Hippocampal volume <sup>d</sup>	ILMN_1767816	-1.93	$5.91 \times 10^{-2}$	N/A

<sup>a</sup> Data for 4 participants were unavailable ( $n = 657$ ). T-value and P-values were obtained from linear regression analysis with adjustment of age, sex, intracranial volumes, and MRI field strength

<sup>b</sup> Data for 76 participants were unavailable ( $n = 585$ ). T-value and P-values were obtained from linear regression analysis with adjustment of age and sex

<sup>c</sup> Data for 216 participants were unavailable ( $n = 458$ ). T-value and P-values were obtained from linear regression analysis with adjustment of age, sex, and intracranial volumes

<sup>d</sup> Data for 220 participants were unavailable ( $n = 1115$ ). T-value and P-values were obtained from a linear mixed model with adjustment of age, sex, and intracranial volumes

Abbreviations: ADNI Alzheimer's Disease Neuroimaging Initiative; FDR false discovery rate; Transcript ID transcript identifier of Affymetrix Human Genome U219 Array for ADNI and Illumina Human HT-12 v3 Expression BeadChips for AddNeuroMed

receptor-mediated phagocytosis is dysregulated in AD [8].

*APH1B* gene encodes Aph-1b protein, one of the four subunits (Aph-1, nicastrin, presenilin, and Pen-2) of  $\gamma$ -secretase [41].  $\gamma$ -secretase is present in many human tissues and well known for contributing to the pathogenesis of AD by cleaving APP and catalyzing the formation of A $\beta$  [42]. Humans have two Aph-1 homologs, Aph-1a and Aph-1b [43], which differ in  $\gamma$ -secretase activity and production of longer and shorter A $\beta$  peptides [44]. Compared to Aph-1a  $\gamma$ -secretase complexes, Aph-1b  $\gamma$ -secretase complexes produced more A $\beta$  peptides with higher A $\beta_{1-42/1-40}$  ratio in a mouse AD model [44]. Biochemical evaluation of pathogenic presenilin and APP mutations of familial AD suggested that relative increases in longer A $\beta$  species are more relevant to AD than an absolute increment in total A $\beta$  load [45]. It is known that human *APH1B* is more expressed in the blood than in the brain (<https://www.proteinatlas.org>) [46]. Our study showed that expression levels of *APH1B* increased in the blood of AD patients and eQTL of *APH1B* in the blood is one of 29 AD-associated SNPs from a recent large-scale

AD GWAS meta-analysis [3]. SMR analysis also validated the causal effect of blood *APH1B* expression on AD. It suggests the possibility that A $\beta$  peptides with higher A $\beta_{1-42/1-40}$  ratio might be produced in the blood and transported into the brain in AD patients, which could be implicated in the pathogenesis of AD. Of note, *APH1B* was suggested as a causal gene of AD in a recent large-scale genome-wide meta-analysis [47].

Higher expression levels of *APH1B* were associated with lower plasma levels of growth hormone receptors, which decreased in patients with MCI and AD compared to CN. The effects of growth hormone are exerted by binding to the growth hormone receptors on target cells, which stimulate the production and secretion of insulin-like growth factor 1 (IGF-1) from the liver and other tissues [48]. The deficits in IGF-1 signaling have been related to AD pathology such as increased accumulation of A $\beta$ , phosphorylated tau, increased neuroinflammation, and apoptosis [49]. Despite evidence for the involvement of the IGF-1 signaling pathway, the human growth hormone secretagogue failed to show efficacy for slowing the rate of progression of AD in a previous clinical trial

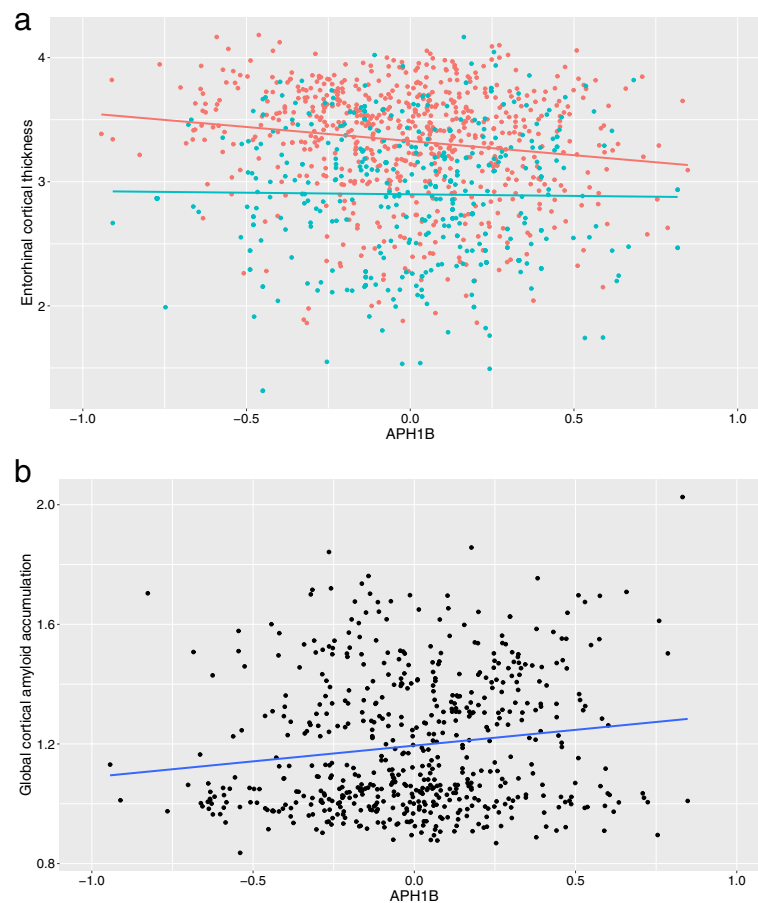


**Fig. 2** Relationship between the blood expression levels of *APH1B* and neuroimaging biomarkers. The association of the blood expression levels of *APH1B* with entorhinal cortical thickness (**a**) and averaged cortical uptake of [ $^{18}$ F] florbetapir PET (**b**) was represented in the scatter plot. In panel **a**, the orange and light blue dots denote data from ADNI and AddNeuroMed, respectively. The orange and light blue lines were obtained from a linear regression analysis in ADNI and AddNeuroMed, respectively. In panel **b**, the black dots denote data from ADNI and the dark blue line was obtained from a linear regression analysis. The gray zones around the lines indicate a 95% confidence interval. The transcript identifier for *APH1B* was 11720068\_a\_at in ADNI and ILMN\_1767816 in AddNeuroMed, respectively. Abbreviation: ADNI, Alzheimer's Disease Neuroimaging Initiative

[50]. Decreased plasma levels of growth hormone receptors in patients with MCI and AD from our study might be related to deficits in the IGF-1 signaling pathway in AD. In addition, the growth hormone receptor is known to be one of the  $\gamma$ -secretase substrates [51], which might explain the relationship between decreased plasma levels of growth hormone receptors and increased expression levels of *APH1B* in our study.

### Limitations

This study has some limitations. First, as eQTL analysis identified and replicated seven AD target genes, we could use only seven genes in the pathway enrichment analysis. Although there is no general rule regarding the number of genes, a list of tens or hundreds of genes is commonly used for enrichment analysis. Second, blood-based RNA

expression profiles could be influenced by confounding factors such as medication, as well as blood collection, processing, and storage procedures. The transcriptomic samples in the ADNI and AddNeuroMed cohorts were, however, collected, processed, and stored following the standard protocols to minimize these risks [52]. Third, RNA expression profiling was performed on different microarray platforms in the ADNI and AddNeuroMed cohorts. Therefore, we did not perform a mega-analysis but used two cohorts as discovery and replication samples in this study. Fourth, as amyloid biomarkers were not available in AddNeuroMed, the association of expression levels of *APH1B* with brain amyloid deposition was investigated in only ADNI.

**Table 4** Association of plasma biomarkers with the expression levels of *APH1B* and their different levels between AD, MCI, and CN in AddNeuroMed

Protein	$T_{APH1B}$	$P_{APH1B}$	$T_{MCI}$	$P_{MCI}$	$T_{AD}$	$P_{AD}$
Neuropilin-1	3.95	$9.69 \times 10^{-5}$	-0.0657	$9.48 \times 10^{-1}$	0.845	$3.99 \times 10^{-1}$
Tropomyosin receptor kinase A	3.76	$2.00 \times 10^{-4}$	-0.571	$5.68 \times 10^{-1}$	1.54	$1.24 \times 10^{-1}$
Growth hormone receptor	-3.59	$3.80 \times 10^{-4}$	-2.44	$1.51 \times 10^{-2}$	-3.25	$1.29 \times 10^{-3}$
Apolipoprotein A1	-3.53	$4.82 \times 10^{-4}$	-0.448	$6.54 \times 10^{-1}$	-1.09	$2.78 \times 10^{-1}$

Data for 344 participants were unavailable.  $T_{APH1B}$  and  $P_{APH1B}$  values were obtained from linear regression analysis for the expression levels of *APH1B* with adjustment of age and sex. Results with uncorrected  $P < 0.001$  are presented.  $T_{MCI}$ ,  $T_{AD}$ ,  $P_{MCI}$ , and  $P_{AD}$  were obtained from analysis of covariance for diagnosis group (CN, MCI, and AD) with adjustment of age and sex

**Abbreviations:** AD Alzheimer's disease; CN cognitively normal older adults; MCI mild cognitive impairment;  $P_{APH1B}$  P-value for *APH1B* expression in linear regression analysis;  $P_{AD}$  P-value for AD diagnosis in the analysis of covariance;  $P_{MCI}$  P-value for MCI diagnosis in the analysis of covariance;  $T_{APH1B}$  T-value for *APH1B* expression in linear regression analysis;  $T_{AD}$  T-value for AD diagnosis in the analysis of covariance;  $T_{MCI}$  T-value for MCI diagnosis in the analysis of covariance

## Conclusions

In summary, our results show that dysregulated expression levels of *APH1B* in peripheral blood are associated with brain atrophy and A $\beta$  deposition in AD. Considering the complex interaction between the brain and the periphery, *APH1B* expression levels in the blood might play a role in the pathogenesis of AD. Although  $\gamma$ -secretase has been a target for therapeutic development for AD, all of the  $\gamma$ -secretase inhibitors until now have failed to show efficacy in clinical trials [53]. Because  $\gamma$ -secretase cleaves more than 100 substrates besides APP [54], it would be extremely difficult to obtain a safe therapeutic window with blocking indiscriminately all different  $\gamma$ -secretase complexes [45]. Previously, selective targeting of Aph-1b  $\gamma$ -secretase complexes was suggested as an effective treatment option for AD [44]. Deficiency of Aph-1a was associated with reduced  $\gamma$ -secretase activity, whereas deficiency of Aph-1b was not, which indicates that Aph-1b  $\gamma$ -secretase complexes may fulfill redundant functions [43]. Replication analysis in independent larger cohorts and a functional study of *APH1B* and its implication for AD treatment are warranted.

## Supplementary Information

The online version contains supplementary material available at <https://doi.org/10.1186/s13195-021-00919-z>.

**Additional file 1: Supplementary Table S1.** Blood eQTL data generated from GWAS genotyping and blood-based RNA expression data in ADNI. **Supplementary Table S2.** Blood eQTL data generated from GWAS genotyping and blood-based RNA expression data in AddNeuroMed. **Supplementary Table S3.** Results of differential gene expression analysis between AD, MCI and CN in ADNI

**Additional file 2: Supplementary Figure S1.** GWAS quality control procedures for samples in the Alzheimer's Disease Neuroimaging Initiative cohort. **Supplementary Figure S2.** Quality control procedures of mRNA expression data for samples in the Alzheimer's Disease Neuroimaging Initiative cohort

## Acknowledgements

This work was supported by the National Research Foundation of Korea grant funded by the Korean government (Ministry of Science and ICT) (No. 2020R1C1C1013718). The Medical Research Collaborating Center of Seoul National University Bundang Hospital contributed to statistical analyses.

## Authors' contributions

YHP and KN designed the study. AH, AJS, and KN collected the data. YHP, JMP, JWJ, SK, and KN interpreted and analyzed the data. YHP and KN drafted the initial manuscript. YHP, PJB, and KN revised the manuscript. The authors read and approved the final manuscript.

## Funding

Data collection and sharing for this project was funded by the Alzheimer's Disease Neuroimaging Initiative (National Institutes of Health Grant U01 AG024904) and DOD ADNI (Department of Defense award number W81XWH-12-2-0012). ADNI is funded by the National Institute on Aging, the National Institute of Biomedical Imaging and Bioengineering, and through generous contributions from the following: AbbVie, Alzheimer's Association; Alzheimer's Drug Discovery Foundation; Araclon Biotech; BioClinica, Inc.; Biogen; Bristol-Myers Squibb Company; CereSpir, Inc.; Cogstate; Eisai Inc.; Elan Pharmaceuticals, Inc.; Eli Lilly and Company; EuroImmun; F. Hoffmann-La Roche Ltd. and its affiliated company Genentech, Inc.; Fujirebio; GE Healthcare; IXICO Ltd.; Janssen Alzheimer Immunotherapy Research & Development, LLC.; Johnson & Johnson Pharmaceutical Research & Development LLC.; Lumosity; Lundbeck; Merck & Co., Inc.; Meso Scale Diagnostics, LLC.; NeuroRx Research; Neurotrack Technologies; Novartis Pharmaceuticals Corporation; Pfizer Inc.; Piramal Imaging; Servier; Takeda Pharmaceutical Company; and Transition Therapeutics. The Canadian Institutes of Health Research is providing funds to support ADNI clinical sites in Canada. Private sector contributions are facilitated by the Foundation for the National Institutes of Health ([www.fnih.org](http://www.fnih.org)). The grantee organization is the Northern California Institute for Research and Education, and the study is coordinated by the Alzheimer's Therapeutic Research Institute at the University of Southern California. ADNI data are disseminated by the Laboratory for Neuro Imaging at the University of Southern California. The collection and analysis of AddNeuroMed samples was supported by InnoMed (Innovative Medicines in Europe) an Integrated Project funded by the European Union of the Sixth Framework program priority FP6-2004-LIFESCIHEALTH-5, the Alzheimer's Research Trust, the John and Lucille van Geest Foundation, and the NIHR Biomedical Research Centre for Mental Health at the South London and Maudsley NHS Foundation Trust and [Institute of Psychiatry] Kings College London.

Additional support for data analysis was provided by NLM R01 LM012535, NIA R03 AG054936, NIA R01 AG19771, NIA P30 AG10133, NLM R01 LM011360, DOD W81XWH-14-2-0151, NIGMS P50GM115318, NCATS UL1 TR001108, NIA K01 AG049050, NIA U01 AG068057, NIA U01 AG072177, NIA U01 AG24904, the Alzheimer's Association, the Indiana Clinical and Translational Science Institute, and the IU Health-IU School of Medicine Strategic Neuroscience Research Initiative.

### Availability of data and materials

The datasets used and/or analyzed during the current study are available from the corresponding author on reasonable request.

Data used in the preparation of this article were obtained from the Alzheimer's Disease Neuroimaging Initiative (ADNI) database ([adni.loni.usc.edu](http://adni.loni.usc.edu)). As such, the investigators within the ADNI contributed to the design and implementation of ADNI and/or provided data but did not participate in the analysis or writing of this report. A complete listing of ADNI investigators can be found at [http://adni.loni.usc.edu/wp-content/uploads/how\\_to\\_apply/ADNI\\_Acknowledgement\\_List.pdf](http://adni.loni.usc.edu/wp-content/uploads/how_to_apply/ADNI_Acknowledgement_List.pdf).

### Declarations

#### Ethics approval and consent to participate

Written informed consent was obtained at the time of enrollment and included permission for analysis and data sharing. The protocol and informed consent forms were approved by the Institutional Review Board at each participating site.

#### Consent for publication

Not applicable.

#### Competing interests

Prof. SangYun Kim is a member of *Alzheimer's Research & Therapy's* editorial board.

#### Author details

<sup>1</sup>Department of Neurology, Seoul National University Bundang Hospital and Seoul National University College of Medicine, Seongnam, Republic of Korea. <sup>2</sup>Department of Neurology, Uijeongbu Eulji Medical Center, Eulji University, Uijeongbu, Republic of Korea. <sup>3</sup>Institute of Psychiatry, Psychology & Neuroscience, King's College London, London, UK. <sup>4</sup>Department of Neurology, Kangwon National University Hospital, Chuncheon, Republic of Korea. <sup>5</sup>Department of Radiology and Imaging Sciences, and the Indiana Alzheimer Disease Center, Center for Neuroimaging, Indiana University School of Medicine, Indianapolis, IN, USA. <sup>6</sup>Department of Medical and Molecular Genetics, Indiana University School of Medicine, Indianapolis, IN, USA. <sup>7</sup>Center for Computational Biology and Bioinformatics, Indiana University School of Medicine, Indianapolis, IN, USA.

Received: 20 June 2021 Accepted: 18 October 2021

Published online: 03 November 2021

### References

- Gatz M, Reynolds CA, Fratiglioni L, Johansson B, Mortimer JA, Berg S, et al. Role of genes and environments for explaining Alzheimer disease. *Arch Gen Psychiatry*. 2006;63:168–74.
- Bellenguez C, Grenier-Boley B, Lambert J-C. Genetics of Alzheimer's disease: where we are, and where we are going. *Curr Opin Neurobiol*. 2020;61:40–8.
- Jansen IE, Savage JE, Watanabe K, Bryois J, Williams DM, Steinberg S, et al. Genome-wide meta-analysis identifies new loci and functional pathways influencing Alzheimer's disease risk. *Nat Genet*. 2019;9:404–13.
- Wang J, Gu BJ, Masters CL, Wang Y-J. A systemic view of Alzheimer disease - insights from amyloid- $\beta$  metabolism beyond the brain. *Nat Rev Neurol*. 2017;13:612–23.
- Selkoe DJ, Hardy J. The amyloid hypothesis of Alzheimer's disease at 25 years. *EMBO Mol Med*. 2016;8:595–608.
- Roher AE, Esh CL, Kokjohn TA, Castaño EM, Vickle GDV, Kalback WM, et al. Amyloid beta peptides in human plasma and tissues and their significance for Alzheimer's disease. *Alzheimers Dement*. 2009;5:18–29.
- Nicolae DL, Gamazon E, Zhang W, Duan S, Dolan ME, Cox NJ. Trait-associated SNPs are more likely to be eQTLs: annotation to enhance discovery from GWAS. *PLoS Genet*. 2010;6:e1000888.
- Park YH, Hodges A, Risacher SL, Lin K, Jang JW, Ahn S, et al. Dysregulated fc gamma receptor-mediated phagocytosis pathway in Alzheimer's disease: network-based gene expression analysis. *Neurobiol Aging*. 2020;88:24–32.
- Aisen PS, Petersen RC, Donohue M, Weiner MW, Initiative ADN. Alzheimer's Disease Neuroimaging Initiative 2 clinical Core: progress and plans. *Alzheimers Dement*. 2015;11:734–9.
- Lovestone S, Francis P, Kloszewska I, Mecocci P, Simmons A, Soininen H, et al. AddNeuroMed--the European collaboration for the discovery of novel biomarkers for Alzheimer's disease. *Ann NY Acad Sci*. 2009;1180:36–46.
- McKhann G, Drachman D, Folstein M, Katzman R, Price D, Stadlan EM. Clinical diagnosis of Alzheimer's disease: report of the NINCDS-ADRDA work group under the auspices of Department of Health and Human Services Task Force on Alzheimer's disease. *Neurology*. 1984;34:939–44.
- Saykin AJ, Shen L, Yao X, Kim S, Nho K, Risacher SL, et al. Genetic studies of quantitative MCI and AD phenotypes in ADNI: progress, opportunities, and plans. *Alzheimers Dement*. 2015;11:792–814.
- Proitsi P, Lupton MK, Velayudhan L, Newhouse S, Fogh I, Tsolaki M, et al. Genetic predisposition to increased blood cholesterol and triglyceride lipid levels and risk of Alzheimer disease: a Mendelian randomization analysis. *PLoS Med*. 2014;11:e1001713.
- Purcell S, Neale B, Todd-Brown K, Thomas L, Ferreira MAR, Bender D, et al. PLINK: a tool set for whole-genome association and population-based linkage analyses. *Am J Hum Genet*. 2007;81:559–75.
- Lee Y, Han S, Kim D, Kim D, Horgosluoglu E, Risacher SL, et al. Genetic variation affecting exon skipping contributes to brain structural atrophy in Alzheimer's disease. *AMIA Jt Summits Transl Sci Proc*. 2017;2018:124–31.
- Price AL, Patterson NJ, Plenge RM, Weinblatt ME, Shadick NA, Reich D. Principal components analysis corrects for stratification in genome-wide association studies. *Nat Genet*. 2006;38:904–9.
- Thorisson GA, Smith AV, Krishnan L, Stein LD. The international HapMap project web site. *Genome Res*. 2005;15:1592–3.
- Li Y, Willer CJ, Ding J, Scheet P, Abecasis GR. MaCH: using sequence and genotype data to estimate haplotypes and unobserved genotypes. *Genet Epidemiol*. 2010;34:816–34.
- McCarthy S, Das S, Kretzschmar W, Delaneau O, Wood AR, Teumer A, et al. A reference panel of 64,976 haplotypes for genotype imputation. *Nat Genet*. 2016;48:1279–83.
- Voyle N, Keohane A, Newhouse S, Lunnon K, Johnston C, Soininen H, et al. A pathway based classification method for analyzing gene expression for Alzheimer's disease diagnosis. *J Alzheimers Dis*. 2016;49:659–69.
- Choe SE, Boutros M, Michelson AM, Church GM, Halfon MS. Preferred analysis methods for Affymetrix GeneChips revealed by a wholly defined control dataset. *Genome Biol*. 2005;6:R16.
- Du P, Kibbe WA, Lin SM. Lum: a pipeline for processing Illumina microarray. *Bioinformatics*. 2008;24:1547–8.
- Schadt EE, Schadt EE, Woo S, Hao K. Bayesian method to predict individual SNP genotypes from gene expression data. *Nat Genet*. 2012;44:603–8.
- Benjamini Y, Hochberg Y. Controlling the false discovery rate - a practical and powerful approach to multiple testing. *J R Stat Soc Series B Stat Methodol*. 1995;57:289–300.
- Ashburner M, Ball CA, Blake JA, Botstein D, Butler H, Cherry JM, et al. Gene ontology: tool for the unification of biology. *Nat Genet*. 2000;25:25–9.
- The Gene Ontology Consortium. The gene ontology resource: 20 years and still GOing strong. *Nucleic Acids Res*. 2019;47:D330–8.
- Kuleshov MV, Jones MR, Rouillard AD, Fernandez NF, Duan Q, Wang Z, et al. Enrichr: a comprehensive gene set enrichment analysis web server 2016 update. *Nucleic Acids Res*. 2016;44:W90–7.
- Zhu Z, Zhang F, Hu H, Bakshi A, Robinson MR, Powell JE, et al. Integration of summary data from GWAS and eQTL studies predicts complex trait gene targets. *Nat Genet*. 2016;48:481–7.
- Vösa U, Claringbould A, Westra HJ, Bonder MJ, Deelen P, Zeng B, et al. Unraveling the polygenic architecture of complex traits using blood eQTL meta-analysis. *Biorxiv*. 2018;447367.
- Jack CR, Bernstein MA, Borowski BJ, Gunter JL, Fox NC, Thompson PM, et al. Update on the magnetic resonance imaging core of the Alzheimer's disease neuroimaging initiative. *Alzheimers Dement*. 2010;6:212–20.
- Risacher SL, Kim S, Nho K, Foroud T, Shen L, Petersen RC, et al. APOE effect on Alzheimer's disease biomarkers in older adults with significant memory concern. *Alzheimers Dement*. 2015;11:1417–29.
- Sattler M, Kiddle SJ, Newhouse S, Proitsi P, Nelson S, Williams S, et al. Alzheimer's disease biomarker discovery using SOMAscan multiplexed protein technology. *Alzheimers Dement*. 2014;10:724–34.

33. Shimohama S. Apoptosis in Alzheimer's disease—an update. *Apoptosis*. 2000;5:9–16.
34. Bukhari H, Glotzbach A, Kolbe K, Leonhardt G, Looose C, Müller T. Small things matter: implications of APP intracellular domain AICD nuclear signaling in the progression and pathogenesis of Alzheimer's disease. *Prog Neurobiol*. 2017;156:189–213.
35. Pallister C, Jung SS, Shaw I, Nalbantoglu J, Gauthier S, Cashman NR. Lymphocyte content of amyloid precursor protein is increased in Down's syndrome and aging. *Neurobiol Aging*. 1997;18:97–103.
36. Leuner K, Pantel J, Frey C, Schindowski K, Schulz K, Wegat T, et al. Enhanced apoptosis, oxidative stress and mitochondrial dysfunction in lymphocytes as potential biomarkers for Alzheimer's disease. *J Neural Transm Suppl*. 2007;96:207–15.
37. Marsh SE, Abud EM, Lakatos A, Karimzadeh A, Yeung ST, Davtyan H, et al. The adaptive immune system restrains Alzheimer's disease pathogenesis by modulating microglial function. *Proc Natl Acad Sci U S A*. 2016;113:E1316–25.
38. Choi ML, Gandhi S. Crucial role of protein oligomerization in the pathogenesis of Alzheimer's and Parkinson's diseases. *FEBS J*. 2018;285:3631–44.
39. Wang MJ, Yi S, Han J, Park SY, Jang JW, Chun IK, et al. Oligomeric forms of amyloid- $\beta$  protein in plasma as a potential blood-based biomarker for Alzheimer's disease. *Alzheimers Res Ther*. 2017;9:98.
40. Youn YC, Kang S, Suh J, Park YH, Kang MJ, Pyun J-M, et al. Blood amyloid- $\beta$  oligomerization associated with neurodegeneration of Alzheimer's disease. *Alzheimers Res Ther*. 2019;11:40.
41. Gertsik N, Chiu D, Li Y-M. Complex regulation of  $\gamma$ -secretase: from obligatory to modulatory subunits. *Front Aging Neurosci*. 2014;6:342.
42. Francis R, McGrath G, Zhang J, Ruddy DA, Sym M, Apfeld J, et al. Aph-1 and pen-2 are required for notch pathway signaling, gamma-secretase cleavage of betaAPP, and presenilin protein accumulation. *Dev Cell*. 2002;3:85–97.
43. Shirovani K, Edbauer D, Prokop S, Haass C, Steiner H. Identification of distinct gamma-secretase complexes with different APH-1 variants. *J Biol Chem*. 2004;279:41340–5.
44. Serneels L, Biervliet JV, Craessaerts K, Dejaegere T, Horr  K, Houtvin TV, et al. Gamma-Secretase heterogeneity in the Aph1 subunit: relevance for Alzheimer's disease. *Science*. 2009;324:639–42.
45. Voytyuk I, De Strooper B, Ch vez-Guti rrez L. Modulation of  $\gamma$ - and  $\beta$ -secretases as early prevention against Alzheimer's disease. *Biol Psychiatry*. 2018;83:320–7.
46. Uhl n M, Fagerberg L, Hallstr m BM, Lindskog C, Oksvold P, Mardinoglu A, et al. Tissue-based map of the human proteome. *Science*. 2015;347:394.
47. Schwartzentruber J, Cooper S, Liu JZ, Barrio-Hernandez I, Bello E, Kumazaki N, et al. Genome-wide meta-analysis, fine-mapping and integrative prioritization implicate new Alzheimer's disease risk genes. *Nat Genet*. 2021;53:392–402.
48. Dehkhoda F, Lee CMM, Medina J, Brooks AJ. The growth hormone receptor: mechanism of receptor activation, cell signaling, and physiological aspects. *Front Endocrinol*. 2018;9:35.
49. Bedse G, Domenico FD, Serviddio G, Cassano T. Aberrant insulin signaling in Alzheimer's disease: current knowledge. *Front Neurosci*. 2015;9:204.
50. Sevigny JJ, Ryan JM, van Dyck CH, Peng Y, Lines CR, Nessler ML, et al. Growth hormone secretagogue MK-677: no clinical effect on AD progression in a randomized trial. *Neurology*. 2008;71:1702–8.
51. Cowan JW, Wang X, Guan R, He K, Jiang J, Baumann G, et al. Growth hormone receptor is a target for presenilin-dependent gamma-secretase cleavage. *J Biol Chem*. 2005;280:19331–42.
52. Park YH, Hodges A, Simmons A, Lovestone S, Weiner MW, Kim S, et al. Association of blood-based transcriptional risk scores with biomarkers for Alzheimer disease. *Neurol Genet*. 2020;6:e517–2.
53. Nie P, Vartak A, Li Y-M.  $\gamma$ -Secretase inhibitors and modulators: mechanistic insights into the function and regulation of  $\gamma$ -secretase. *Semin Cell Dev Biol*. 2020;105:43–53.
54. G ner G, Lichtenthaler SF. The substrate repertoire of  $\gamma$ -secretase/presenilin. *Semin Cell Dev Biol*. 2020;105:27–42.

### Publisher's Note

Springer Nature remains neutral with regard to jurisdictional claims in published maps and institutional affiliations.

Ready to submit your research? Choose BMC and benefit from:

- fast, convenient online submission
- thorough peer review by experienced researchers in your field
- rapid publication on acceptance
- support for research data, including large and complex data types
- gold Open Access which fosters wider collaboration and increased citations
- maximum visibility for your research: over 100M website views per year

At BMC, research is always in progress.

Learn more [biomedcentral.com/submissions](https://biomedcentral.com/submissions)

